Anal Bioanal Chem (2016) 408:721–731
DOI 10.1007/s00216-015-9206-0

PAPER IN FOREFRONT

Identification of sirtuin 5 inhibitors by ultrafast microchip electrophoresis using nanoliter volume samples

Erik D. Guetschow[1] · **Surinder Kumar**[2] · **David B. Lombard**[2,3] · **Robert T. Kennedy**[1,4]

Received: 15 October 2015 / Revised: 13 November 2015 / Accepted: 19 November 2015 / Published online: 3 December 2015

Abstract Sirtuin 5 (SIRT5) is a member of the sirtuin family of protein deacylases that catalyzes removal of post-translational modifications, such as succinyl and malonyl moieties, on lysine residues. In light of SIRT5's roles in regulating metabolism, and its reported oncogenic functions, SIRT5 modulators would be valuable tools for basic biological research and perhaps clinically. Several fluorescence assays for sirtuin modulators have been developed; however, the use of fluorogenic substrates has the potential to cause false positive results due to interactions of engineered substrates with enzyme or test compounds. Therefore, development of high-throughput screening (HTS) assays based on other methods is valuable. In this study, we report the development of a SIRT5 assay using microchip electrophoresis (MCE) for identification of SIRT5 modulators. A novel SIRT5 substrate based on succinate dehydrogenase (SDH) was developed to allow rapid and efficient separation of substrate and product peptide. To achieve high throughput, samples were injected onto the microchip using a droplet-based scheme. By coupling this approach to existing HTS sample preparation workflows, 1408 samples were analyzed at 0.5 Hz in 46 min. Using a 250 ms separation time, eight MCE injections could be made from each sample generating >11,000 electropherograms during analysis. Of the 1280 chemicals tested, eight were identified as inhibiting SIRT5 activity by at least 70 % and verified by dose-response analysis.

Keywords Sirtuin · Screening · Electrophoresis · Microfluidics · Droplets

Introduction

Sirtuins are an evolutionarily conserved class of nicotinamide adenine dinucleotide (NAD^+)-dependent deacylases comprised of seven members (SIRT1-SIRT7) [1, 2]. The SIRT mediated deacylase reaction consumes NAD^+ generating a deacylated product, 2′-O-acyl-ADP-ribose, and nicotinamide. Recent research has revealed novel catalytic functions for sirtuins, such as deacylation [3, 4], desuccinylation [5–8], deglutarylation [9], demalonylation [7, 10], and decrotonylation [11], with SIRT5 preferentially targeting succinyl, glutaryl, and malonyl moieties [5–10, 12]. Through removal of these modifications, SIRT5 regulates the activity of many metabolic enzymes, such as carbamoyl phosphate synthetase 1 (CPS1) [13, 14], superoxide dismutase 1 (SOD1) [15], succinate dehydrogenase (SDH) [12], pyruvate dehydrogenase complex (PDC) [12], and 3-hydroxyl-3-methylglutaryl-CoA synthase 2 (HMGCS2) [8]. SIRT5 regulates glycolysis through demalonylation of glyceraldehyde 3-phosphate dehydrogenase (GAPDH) and aldolase B, among other targets [10]. SIRT5 knockout cells show extensive hypersuccinylation. Although no striking biological phenotype or abnormality is observed for SIRT5 knockout cell lines [16], SIRT5 may play a role in cancer biology [17, 18] as

Electronic supplementary material The online version of this article (doi:10.1007/s00216-015-9206-0) contains supplementary material, which is available to authorized users.

✉ Robert T. Kennedy
rtkenn@umich.edu

[1] Department of Chemistry, University of Michigan, 930 N University Ave, Ann Arbor, MI 48109, USA

[2] Department of Pathology, University of Michigan, 1301 Catherine St, Ann Arbor, MI 48109, USA

[3] Institute of Gerontology, University of Michigan, 300 N Ingalls St, Ann Arbor, MI 48109, USA

[4] Department of Pharmacology, University of Michigan, 1150 W. Medical Center Dr., Ann Arbor, MI 48109, USA

suggested by its overexpression and reported pro-proliferative role in lung cancer cells [15, 19].

Because of the diverse roles that SIRT5 plays within cells, identification of small molecule modulators of SIRT5 activity could have biological and clinical applications. Development of robust HTS assays for SIRT5 is necessary to enable rapid testing and identification of modulators. To date, much work has been done screening other members of the sirtuin family through optical assays, such as the commercially available *Fluor-de-Lys* assay based on 7-amino-4-methylcoumarin (AMC) [20–24]. After catalytic removal of the lysine modification by a sirtuin, the AMC probe is accessible to cleavage by trypsin leading to an increase in fluorescent signal [25]. This type of assay was used for the identification of sirtuin 1 activators reported to increase lifespan in invertebrates and in mice [21, 26, 27]. While these assays are amenable to HTS, the close proximity of dye molecule and lysine residue has resulted in artifactual results during screening [20, 28, 29]. To avoid these limitations, groups have developed alternative assays for SIRT5 screening based on optical detection of nicotinamide formation [30], inclusion of fluorophore-quencher pairs in the substrate [31], high-performance liquid chromatography-mass spectrometry (HPLC-MS) [5, 32, 33], and fluorescence-resonance energy transfer [34]. However, the number of compounds screened has been limited and the throughput required for large-scale screening has not been demonstrated.

Previously, electrophoresis assays have been used for screening of sirtuins [35–40], GTPase [41], and other enzymes [42, 43]. Although these assays typically use fluorescent substrates, the label is often located remote from the target residue, reducing the likelihood of false positives due to nonspecific interactions. Conventional capillary (CE) or microchip electrophoresis (MCE) methods use auto-samplers or manual sample loading leading to a maximum throughput of a few samples per minute.

Droplet-based sample introduction for CE and MCE has recently been demonstrated for screening [41, 44] and other assays [45–49] as a way to improve sample introduction to microfluidic devices. Indeed, we previously developed a droplet-MCE assay for protein kinase A (PKA) capable of analyzing eight samples per min [44]. Due to the small number of compounds tested in these screens, the method robustness required for routine high-throughput analysis has not been demonstrated. Herein we report the use of droplet-MCE with 3-fold improved throughput over prior studies for a screen of 1280 compounds against SIRT5.

Experimental

Chemicals and materials

Unless otherwise specified, all reagents were purchased from Sigma Aldrich (St. Louis, MO, USA). SDHA-derived peptide was synthesized by GenicBio Ltd, (Shanghai, China). All test compounds were from the Prestwick Chemical Library (Prestwick Chemical, Washington DC, USA) and were supplied by the Center for Chemical Genomics at the University of Michigan or from the Epigenetics Screening Library (Cayman Chemical, Ann Arbor, MI, USA).

Microfluidic device fabrication

Polydimethylsiloxane (PDMS) droplet extraction devices were prepared using a pour over method as previous described [44]. Glass microfluidic devices were fabricated using photolithography and wet chemical etching by hydrofluoric acid [50–52]. Each device is fabricated from two etched pieces of glass that are aligned prior to bonding. One slide was etched to 80 μm for the capillary insertion channel and sample channel. The second slide was etched to 80 μm for capillary insertion and 3 μm for separation channels. During etching of deep channels, other features were covered with HF resistant tape (Semiconductor Equipment Corporation, Moorpark, CA, USA). After etching, fluidic access holes were made with a 0.5 mm drill bit (Kyocera Tycom, Costa Mesa, CA, USA). Glass slides were washed for 20 min in piranha solution (sulfuric acid:hydrogen peroxide, 4:1) and for 40 min in heated RCA solution (ammonium hydroxide:hydrogen peroxide:water, 1:1:5). Slides were rinsed with water, channels were aligned under a microscope, and bonded at 610 °C for 8 h. Reservoirs (IDEX Health and Science, Oak Harbor, WA, USA) were attached at the access holes using epoxy and a 30 μm i.d. × 150 μm o.d. × 1 mm long extraction capillary was waxed in place in the capillary insertion channel.

Droplet generation from multiwell plate

Droplet formation followed the procedure previously published [53]. Droplets segmented by perfluorodecalin (PFD) were generated from modified polypropylene 384-well plates (Nunc ShallowWell; Thermo Scientific, Waltham, MA, USA) and collected into 150 μm i.d. × 360 μm o.d. HPFA+ tubing (IDEX Health and Science, Oak Harbor, WA, USA). Well height across the entire plate was reduced by 1.5 mm using a CNC milling machine allowing samples to be covered by carrier oil to prevent evaporation and aspiration of air bubbles. For droplet formation, multiwell plate (MWP) and tubing were mounted onto a computer controlled XYZ-positioner so that the tubing inlet could move freely above the wells. The tubing outlet was connected to a 100 μL syringe mounted in a PHD 200 syringe pump (Harvard Apparatus, Holliston, TX, USA) and both were primed with PFD to remove any air bubbles [54]. With the syringe pump operating in refilling mode (1000 nL/min), the tubing inlet was moved from well to well in programmed pattern to generate droplets at 0.75 droplets per second. Briefly, the computer was programmed to move at 2000 mm/s, which was the maximum rate of linear

motion. For each sample droplet, the tubing would dwell in the aqueous phase (420 ms) and in the oil layer (150 ms). Additional oil phase would be aspirated as the tubing moved from well to well. The final droplet volume was 8.2±0.3 nL and each oil spacer was 10.0±0.4 nL. After formation of droplets, a short oil plug (~10 mm) is aspirated into the tube to prevent sample loss caused by flow induced when making connections.

Microchip electrophoresis analysis with droplet samples

Prior to each experiment, all fluidic channels were filled with separation buffer (10 mM sodium tetraborate, pH 10) ensuring that no air bubbles remained. Positive (+2 kV) and negative (–3 kV) high voltage (CZE1000R; Spellman, Hauppauge, NY, USA) was applied to the microfluidic device via platinum electrodes at the fluid reservoirs. Sample was electrokinetically injected [55, 56] for 15 ms using a high-voltage relay (Kilovac; Santa Barbara, Cam USA) controlled by an in-house LabVIEW program (National Instruments, Austin, TX, USA). Detection was accomplished using a confocal laser-induced fluorescence detector. Briefly, a 488 nm line from a solid state laser (CrystaLaser, Reno, NV, USA) was directed through a 488±10 nm band pass filter and reflected by a 500 nm dichroic mirror into a 40X objective lens. Emitted light was collected by the same objective and passed through the dichroic mirror. The emitted light was filtered through a 520±10 nm band pass filter and 400 μm pinhole prior to being detected by a photomultiplier tube (R1477; Hamamatsu, Bridgewater, NJ, USA). Current from the PMT was amplified (SR570 current preamplifier; Stanford Research Systems, Sunnyvale, CA, USA) and monitored using in-house LabVIEW control software. Data were sampled at 1000 Hz using a 16-bit data acquisition card (PCI-6036E; National Instruments Corp., Austin, TX, USA). Electropherograms were analyzed with Cutter 7.0 [57]. Statistical analysis and plotting were done in Excel 2011 (Microsoft, Redmond, WA, USA), and Igor Pro 6.32 (Wavemetrics, Inc., Lake Oswego, OR, USA).

Droplet samples were introduced as outlined previously. A length of tubing containing sample droplets connected to a 100 μL syringe via a union and the outlet was inserted in to the PDMS extraction device at a 90° angle to the extraction capillary inlet. Downstream of the extraction region, a 40 μm i.d. × 150 μm o.d. fused silica capillary connected to a 100 μL syringe is inserted into the device to generate waste droplets that promote extraction by increasing backpressure at the extraction point. Droplets were pumped into the extraction device at 700 nL/min and electrokinetic injections were made at 4 Hz.

In vitro PDC desuccinylation assay

Porcine heart PDC (Sigma Aldrich, St. Louis, MO, USA) was purified by centrifugation at 135,000×*g* for 2 h in 100 mM potassium phosphate, pH 7.5, 0.05 % lauryl maltoside, 2.5 mM EDTA, and 30 % glycerol. Desuccinylation reactions were carried out on 30 μg of purified porcine heart PDC in a final reaction volume of 60 μL in presence of 25 mM Tris-Cl, pH 8.0, 200 mM NaCl, 5 mM KCl, 1 mM MgCl2, 0.1 % PEG 8000, and 3.125 mM NAD^+ at 37 °C for 2 h. Where indicated, 10 μg of SIRT5 or $SIRT5^{H158Y}$ (expressed and purified in-house) was added. During incubation, tubes were occasionally agitated. Following desuccinylation, 15 μL each reaction was analyzed by immunoblotting with a succinyl-lysine antibody (PTM Biolabs Inc., Chicago, IL, USA). After analysis, the membrane was stripped and re-probed for PDHA1 (Abcam, Cambridge, MA, USA) and SIRT5 (Cell Signaling Technology, Danvers, MA, USA).

Peptide-based SIRT5 assay

Assay conditions were developed using a novel succinyl-lysine peptide derived from succinate dehydrogenase [12]. The substrate peptide (GGQSLK[succ]FGKG) was labeled at the N-terminus with 5-carboxyfluorescein (5-FAM) and yielded a desuccinylated peptide (GGQSLKFGKG) as a product. Reactions were performed in 10 mM Tris, pH 8, containing 1 mM dithiothreitol (DTT) with enzyme concentration fixed at 10 nM. Reactions were stopped by dilution with 1.5 volumes of 10 mM sodium tetraborate, pH 10. Kinetic parameters were determined using substrate concentrations ranging from 0 to 50 μM at time points from 0 to 30 min. Kinetics data was fitted using the Michaelis-Menton model in GraphPad Prism 6. Assay conditions were validated using a small-scale screen of the Epigenetics Screening Library.

High-throughput SIRT5 screening

All screens were performed at 10 μL final volume in a modified low volume MWP and were prepared using a MultiDrop Combi (Thermo Scientific, Waltham, MA, USA). A Caliper Life Science Sciclone ALH300 (PerkinElmer, Waltham, MA, USA) was used to deposit 50 nL of 2 mM test compounds into MWPs containing 5 μL of 2X reaction buffer (20 mM Tris, pH 8, 2 mM DTT). To index samples during analysis, 1 μL of 1 μM rhodamine 110 was added to even number columns and 1 μL of water was added to odd number columns. Next, 1 μL of 10 μM peptide was added to all wells and 3 μL of 33 nM SIRT5 was added to initiate reactions. Final reaction conditions were 1 μM peptide, 10 nM SIRT5, and 10 μM test compound with 0.5 % DMSO. Reactions were quenched by addition of 15 μL of 10 mM sodium tetraborate, pH 10, after 30 min incubation at room temperature. Each plate contained 16 negative (0.5 % DMSO) and 16 positive (10 μM anacardic acid) controls for a total of 352 samples per plate. Each sample was reformatted into a single droplet as detailed above. Reaction yield based on substrate and product peak area was

used for data analysis and normalized to positive and negative controls within each row to account for variation in reaction yield. Hit compounds were verified by dose-response analysis from 0.1 to 100 μM (unless otherwise noted on individual plots) and IC_{50} values were calculated from best fit curves using GraphPad Prism 6.

Results and discussion

Development of a SIRT5 screening substrate

Several research groups have developed assays for SIRT5, since it was first reported to remove novel protein post-translational modifications, such as succinyl, malonyl, and glutaryl moieties [5–10, 12]. Based around fluorogenic substrates [20, 21, 23], these assays are amenable to HTS; but, the engineered assay substrates may not always mimic natural substrates well because of their short length and the presence of a bulky fluorescent probe near target residues. To avoid these limitations, assays based on high-pressure liquid chromatography (HPLC) [5], mass spectrometry (MS) [32], or fluorescence resonance energy transfer (FRET) [34] have been developed that use short peptides based on natural SIRT5 substrates.

In developing our electrophoresis assay, we wanted our peptide substrate to have the fluorescent tag remote from the succinyl lysine to reduce potential for false positive results, have a total charge suitable for rapid electrophoretic separation of substrate and product, and be based on a known SIRT5 target to mimic in vivo substrates. Known SIRT5 targets, such as CPS1 [8, 13, 14], PDC [12], SDH [12], and HMGCS2 [8], as well as hypersuccinylated proteins, such as hydroxyacyl-coenzyme A dehydrogenase (HADH) [12], acetyl-coenzyme A acetyltransferase (ACAT) [12], and malate dehydrogenase (MDH) [8] were identified as templates for substrate development. We selected a peptide based on SDHA K179 because of the favorable peptide charge (–2 for substrate, 0 for product) under basic pH used for analysis, although in principle another target could be used for substrates if desired. The length was sufficient to provide distance (five amino acids) between the 5-FAM tag and the target lysine while providing several amino acids on either side of K179 for substrate recognition as demonstrated by other groups [5, 33, 58]. Additionally, total peptide charge was only slightly negative and allowed for short migration times and good separation from the product peptide formed after SIRT5 desuccinylation.

Separation of the substrate and product peptides was achieved in 250 ms due to favorable charge-to-size ratio, high electric field, and short separation distance (see below). Injection of SIRT5 reaction mixture resulted in two peaks in the electropherogram associated with the succinylated substrate and desuccinylated product peptides (Fig. 1a). Removal of the succinyl moiety caused a +2 change in peptide charge resulting in a faster migration time.

To evaluate the quality of our SDHA-derive peptide substrate, we compared the activity of SIRT5 and $SIRT5^{H158Y}$—catalytically inactive SIRT5—with the peptide substrate and full PDC. For the peptide substrate, robust activity, as quantified by product peak area, was observed for SIRT5 with only slight activity observed for $SIRT5^{H158Y}$ (Fig. 1a). Likewise incubation of PDC with SIRT5, but not $SIRT5^{H158Y}$, resulted in decreased succinylation of PDHA1— the catalytic subunit of PDC (Fig. 1b). Therefore, in terms of SIRT5 activity, our SDHA-derived peptide substrate behaved similarly to full PDC.

Improvements to sample throughput for microchip electrophoresis

Analysis of droplet samples by MCE was done using a hybrid PDMS-glass microfluidic device modified from that described

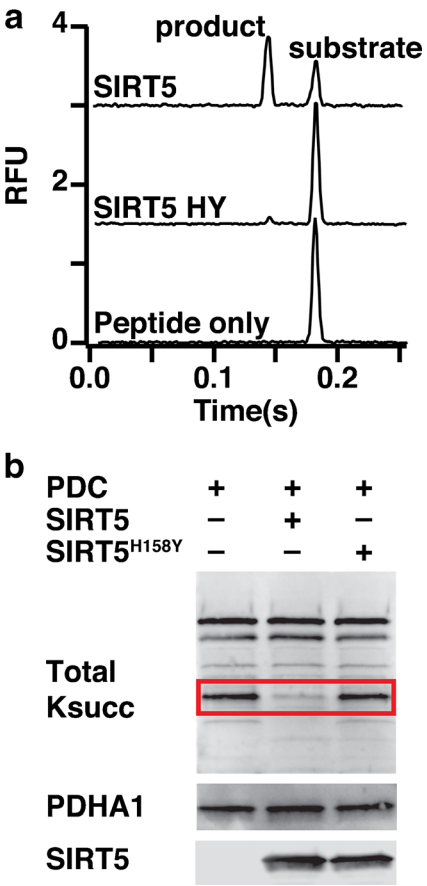

Fig. 1 SIRT5 and $SIRT5^{H158Y}$ have similar activity against SDHA-derived peptide and PDC holoenzyme. **(a)** Electropherograms demonstrating that SIRT5 desuccinylates target peptide forming a product with shorter migration time and that $SIRT5^{H158Y}$ has reduced enzymatic activity. **(b)** Succinylation of porcine heart PDC is reduced following incubation with SIRT5 but not $SIRT5^{H158Y}$. Upper blot: total lysine succinylation; PDHA1 band highlighted in red. Middle and lower blots: PDHA1 and SIRT5, respectively

previously [44] (Fig. 2). In this system, samples stored in a length of Teflon tubing are flowed past the inlet of a fused silica extraction capillary inserted into the glass MCE device. As the droplets exit the Teflon tubing, they are wicked into the extraction capillary. Once on the microfluidic device, they were pulled by EOF toward the voltage-gated injector for MCE analysis (Fig. 2). A combination dead volume in the extraction capillary and separation speed limited the system throughput. In this work, we examined improving the throughput to enable larger scale screens.

In the original system, the extraction capillary had a 3.1 nL volume (2.5 mm length×40 μm i.d.). To effectively clear this dead volume, 16 nL of sample (two droplets of 8 nL each) was required. The time required to perform this rinse limited assay throughput to 0.16 samples per s. For these experiments, the device was redesigned to accommodate a 1 nL extraction capillary (1 mm length×30 μm i.d.). We found that with this volume, a single 8 nL droplet provided a sufficient rinse of the extraction capillary allowing throughput to be increased 2-fold relative to the previous implementation.

Although reduced dead volume increased sample throughput, separation speed remained a bottleneck. In previous work, separation distance was 5 mm and electric field was 2000 V/cm. Using these conditions, rhodamine, substrate, and product for SIRT5 assays were resolved within 1 s (Fig. 3a). Resolution could be maintained at shorter times by reducing detection length and increasing the field (Fig. 3a). The fastest separation achieved was 250 ms at 3500 V/cm and 2 mm separation distance.

At the high field and short separation length, over-injection led to poor resolution. To determine the best injection time, peak variance for substrate and product peptide was measured for injection widths of 10 ms to 35 ms (Fig. 3b). A minimum peak variance was observed at 15 ms injection width for both substrate and product peptides and was used for all future separations. Under these conditions, the average separation

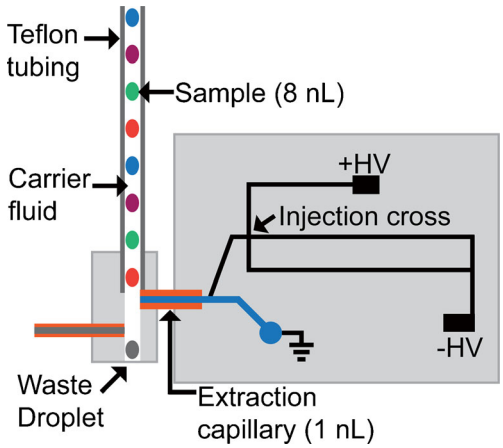

Fig. 2 Schematic of microfluidic device for analysis of droplet samples by MCE showing positioning of droplet samples orthogonally to the 1 mm fused silica extraction capillary

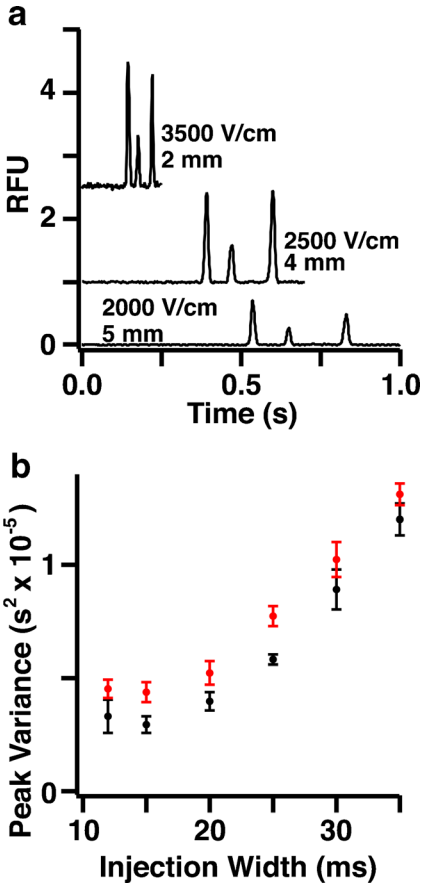

Fig. 3 Separation throughput was increased 4-fold for SIRT5 assay through improvement of separation and injection conditions. **(a)** Electropherograms for initial separation conditions based on previous work and improved conditions capable of baseline separation in as little as 250 ms. **(b)** Optimum injection width is 15 ms based substrate (black) and product (red) peak variance

efficiency for three analytes was 7000±1000 plates. When corrected for analyte migration time, the separation generated 41,000±8 000 theoretical plates/s. These conditions allowed four injections/s so that eight injections were obtained per droplet and sample throughput was 0.5 Hz. This result is a 3-fold increase in sample throughput compared with the previous design [44].

The high rate of injections allowed monitoring of when carryover was eliminated (typically three injections) and collection of at least three replicate assays per droplet. Carryover was determined by monitoring the presence or absence of a rhodamine signal (rhodamine was present in every other droplet) and stability of peak height for substrate and product peaks in the electropherogram.

An important consideration is whether the electropherograms are stable over many injections. Migration time RSD for rhodamine, substrate, and product were 1.3 %, 0.7 %, and 0.6 %, respectively (n=1400). Additionally, peak areas were stable over many injections. For samples containing rhodamine, peak area RSD was less than 5 % for replicate injections

of the same sample (n=3) and average rhodamine peak area RSD was 6 % over 88 samples (n=264 injections). This corresponds to one batch of samples (e.g., 88 samples with rhodamine and 88 without). Slight changes in peak magnitude were observed from batch to batch, but this did not affect data quality because peak area ratios were used for analysis [see Electronic Supporting Material (ESM) Fig. S1 for raw electropherograms from injections made at the beginning and end of the screen]. Substrate and product peak area fluctuated from sample to sample due to slight variation in enzyme efficiency; however, peak area RSD was less than 5 % for replicate injections of the same sample (n=3).

SIRT5 inhibitor screening

The assay for SIRT5 monitored the depletion of substrate peptide (5-FAM-GGQSLK[succ]FGKG) and formation of product peptide (5-FAM-GGQSLKFGKG) simultaneously (Fig. 4a). Reaction yield was normalized to positive and negative controls within each row of the well plate and plotted as normalized SIRT5 activity for each sample. Monitoring two analytes and normalizing to row controls mitigated the effect of variation in sample preparation, injection, or separation efficiency over the course of screening. Samples were indexed by addition of rhodamine 110 to even number samples and monitoring changes in rhodamine peak area to identify samples as previously demonstrated [44]. Prior to screening, substrate concentration for screening was determined from kinetics data. Based on Michaelis-Menton kinetics, the K_m (1.6± 0.4 μM) and K_{cat}/K_m (5.8×10^4 $M^{-1}s^{-1}$) values were determined (Fig. 4b). These match well with reported values for SIRT5 substrate peptides of similar length based on histone H3 (K_m=5.8±2.7 and $K_{cat}/K_m=4.3\times10^3$ $M^{-1}s^{-1}$) [5] and CPS1 (K_m=3.8±0.6 and $K_{cat}/K_m=1.4\times10^4$ $M^{-1}s^{-1}$) [33]. Reaction progress was linear up to 50 min, the longest point tested (Fig. 4c). Addition of 1.5 volumes of 10 mM sodium tetraborate, pH 10, completely inactivates SIRT5 (Fig. 4d). To satisfy screening assay requirements [59, 60] substrate concentration was fixed at 1 μM below the K_m and reactions were quenched after 30 min.

To validate reaction conditions for high throughput screening, SIRT5 activity was screened against a library of 80 compounds from an epigenetics focus library known to inhibit other members of the sirtuin family (see ESM Fig. S2a for SIRT5 pilot screening data). Each test compound was screened at 10 μM. Seven compounds were identified as SIRT5 inhibitors, based on a 50 % inhibition of SIRT5 activity. These hits were verified with dose-response curves and IC_{50} values ranged from 60 nM to 8 μM (see ESM Fig. S2b for pilot screening dose-response curves). Of the compounds, suramin has previously been reported as a SIRT5 inhibitor in NAD^+-nicotinamide exchange assays (IC_{50}=22 μM) [61] and fluorogenic assays (IC_{50}=47 μM) [62]. AGK-2 has been reported as a SIRT5 inhibitor with an IC_{50} value above 100 μM [63]. The difference in IC_{50} values may be due to these assays focusing on SIRT5 deacetylase activity, which is much lower than SIRT5 desuccinylase activity, or differences in assay conditions. The potent inhibitor anacardic acid was chosen as a positive control for future screens based on the results of pilot screening.

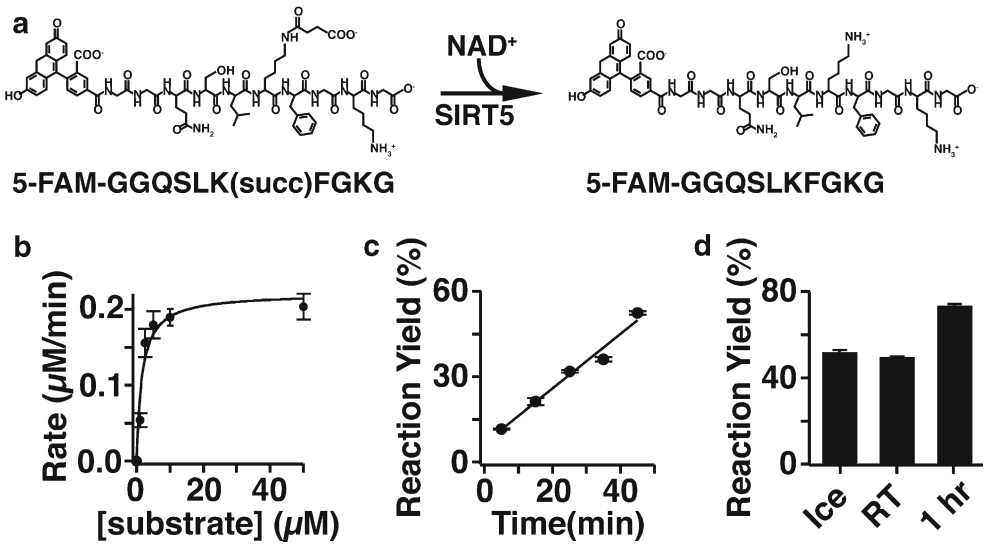

Fig. 4 **(a)** SIRT5 catalyzes the removal of succinyl moieties from lysine side chains in the presence of NAD^+ causing a +2 change in peptide charge. **(b)** Michaelis-Menton kinetics data for SIRT5 with excess NAD^+. K_m is 1.6±0.4 μM, K_{cat} is 0.092±0.008 s^{-1}, and K_{cat}/K_m is 5.8×10^4 $M^{-1}s^{-1}$. **(c)** Reaction progress for 1 μM substrate and 10 nM SIRT5 demonstrating reaction linearity up to ~50 min. **(d)** SIRT5 reaction can be quenched by addition of 1.5 volumes of 10 mM sodium tetraborate, pH 10. Ice sample was quenched after 30 min and stored at –80 °C, RT sample was quenched after 30 min and stored at room temperature, and 1 h sample was allowed to react for 1 h before quenching (n=3 for all samples)

These validated conditions were used to screen the Prestwick Chemical Library, which contains 1280 approved drug compounds, against SIRT5 (Fig. 5a). Reactions were prepared in 384-well plates using high-throughput sample preparation instrumentation for incorporation into existing HTS workflows. Each of the 1408 samples (1280 compounds, 64 positive controls, and 64 negative controls) were reformatted into a single droplet with an average volume of 8.2±0.3 nL (n=352) at 0.75 Hz (although faster reformatting is possible [64]). Analysis was done in batches of 176 samples, corresponding to one-half of a plate, with a sample throughput of 0.5 Hz. Total analysis time was 46 min and generated over 11,000 electropherograms at eight injections per sample (Fig. 5b). The assay Z′-factor, when corrected for row effects caused by sample preparation, was 0.8.

Among the compounds, 10 reduced SIRT5 activity by 70 % and were selected for further study. At the time of initial screening, all reactions containing SIRT5 inhibitors were reformatted as duplicate droplets and analyzed by MCE to confirm results (see Electronic Supporting Material Fig. S3 for inhibition confirmation data). These compounds were evaluated for dose-dependent SIRT5 inhibition and eight were confirmed as SIRT5 inhibitors. The remaining two compounds did not exhibit dose-dependent inhibition of SIRT5 during dose-response analysis and were identified as false-positives caused by sample preparation. All dose-response curves had good fit (R^2>0.90) except antimycin A, which had an IC_{50} value near the maximum tested dose (Fig. 6). The calculated IC_{50} values are in the low micromolar range matching the most potent reported SIRT5 inhibitors [33, 63, 65]. None of the compounds has previously been reported as a SIRT5 inhibitor; however, SIRT5 was reported as a potential target of probucol based on molecular targeting and docking studies [66].

Improvements to sample throughput and robustness

If run continuously, the current system could analyze over 14,000 samples in 8 h; however, even higher throughput may be possible with further improvement. For example, the current separation speed was limited by peak resolution between rhodamine and product peptide, whereas the resolution between product and substrate is 2.5. If rhodamine—used for sample indexing—was replaced by a more positively charged analyte with faster migration velocity, separation time could be further reduced without loss of baseline resolution. For example, reducing separation time to 125 ms (half of the current separation time) could increase sample throughput to 1 Hz (>28,000 samples in 8 h). Additional throughput could be achieved by testing multiple compounds simultaneously [67]. Although additional assays would be needed to de-convolute any inhibitors or synergistic inhibition effects, throughput would increase linearly with the number of compounds per reaction.

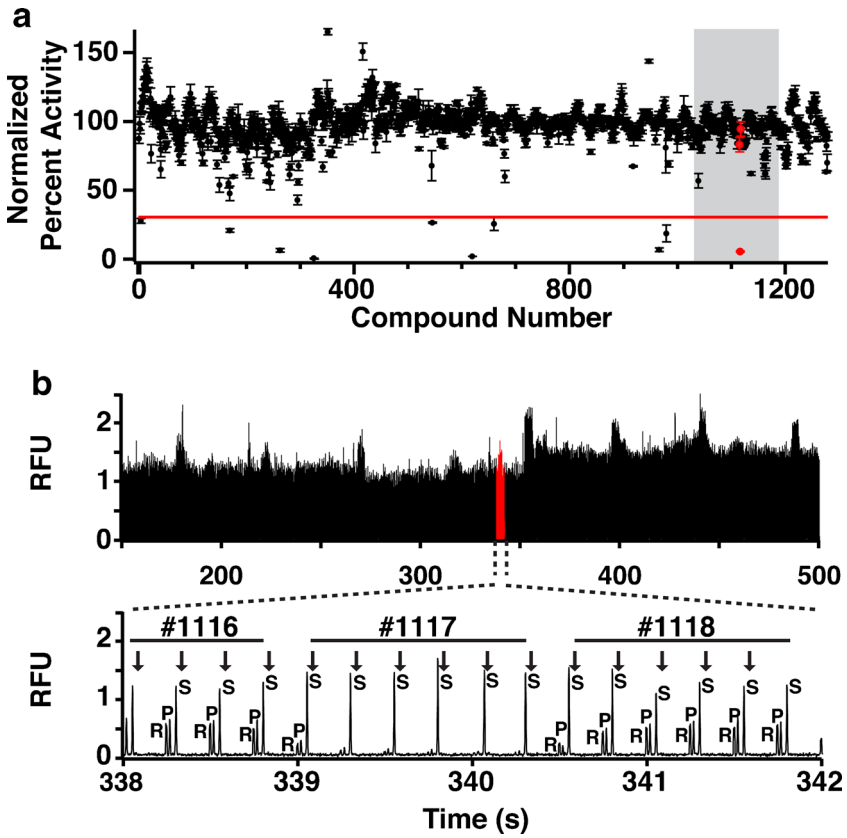

Fig. 5 Screen of Prestwick Collection Library against SIRT5. **(a)** Normalized SIRT5 activity in the presence of 1280 compounds. Each point represents the average SIRT5 activity with a test compound, and a red line denotes the inhibition threshold. **(b)** Top plot: electropherograms corresponding to the 160 compounds in the grey region of Panel A. Bottom plot: enlarged view of red highlighted region (338–342 s) showing separation of rhodamine (R), product (P), and substrate (S) peptides for three compounds. #1117 is an inhibitor. Injections are denoted with an arrow and 6-8 MCE injections are made from each sample droplet

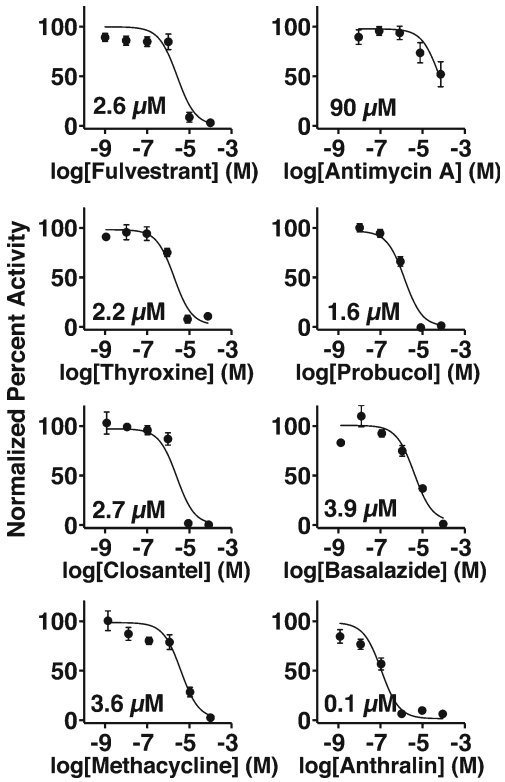

Fig. 6 Dose-response analysis for compounds that reduced SIRT5 activity by >70 %. Ten compounds were identified during screening and eight were confirmed as inhibitors with IC_{50} values provided on each plot

Although we have demonstrated an assay for SIRT5 capable of screening a meso-scale compound library, several factors limit using droplet samples for routine analysis. Several steps during sample analysis require making zero dead volume connections with small flexible tubing, which can be difficult and is labor-intensive. During droplet formation, the number of droplets that can be formed reproducibly is limited by back pressure from droplet samples within the collection tubing. This limits read length to several hundred samples requiring batch analysis for large libraries. Although generating droplets in parallel is possible, it increases complexity and requires additional low dead volume connections [64]. If droplets could be generated and analyzed continuously, analysis limits imposed by low dead volume connections and droplet read length could be mitigated.

Conclusion

In this work, we have described a SIRT5 screening assay based on ultrafast electrophoresis using nanoliter volume samples suitable for meso-scale library screening. A novel SIRT5 substrate derived from SDHA was developed to achieve rapid separation of substrate and product, while avoiding several limitations associated with commercially available fluorogenic substrates. Using this assay, 1408 samples (1280 compounds, 128 controls) were screened against SIRT5, and eight previously unknown SIRT5 inhibitors were identified. Analysis was completed within 46 min (0.5 Hz) and over 11, 000 MCE injections were made demonstrating method speed, robustness, and reliability. Under these conditions, throughput was increased 3-fold relative to previous MCE-based screening and 25-fold compared with previous sirtuin screens by MCE or CE.

Acknowledgments R.T.K and E.D.G were supported by National Institutes of Health grant R01GM102236, the National Institutes of Health Microfluidics in Biomedical Sciences Training Program at University of Michigan T32 EB005582, and the American Chemical Society Division of Analytical Chemistry Graduate Fellowship sponsored by Eli Lilly and Company. D.B.L and S.K. were supported by National Institutes of Health grant R01GM101171, the Glenn Foundation for Medical Research, the National Center for Advancing Translational Sciences of the National Institutes of Health under award UL1TR000433, Department of Defense support for Ovarian Cancer grant OC140123, and the John S. and Suzanne C. Munn Cancer Fund of the University of Michigan Comprehensive Cancer Center.

Compliance with ethical standards

Conflict of interest The authors declare that they have no conflict of interest.

References

1. S-i I, Armstrong CM, Kaeberlein M, Guarente L (2000) Transcriptional silencing and longevity protein Sir2 is an NAD-dependent histone deacetylase. Nature 403(6771):795–800
2. Imai S-i, Guarente L (2010) Ten years of NAD-dependent SIR2 family deacetylases: implications for metabolic diseases. Trends Pharmacol Sci 31(5):212–220
3. Jiang H, Khan S, Wang Y, Charron G, He B, Sebastian C, Du J, Kim R, Ge E, Mostoslavsky R, Hang HC, Hao Q, Lin H (2013) SIRT6 regulates TNF-[agr] secretion through hydrolysis of long-chain fatty acyl lysine. Nature 496(7443):110–113
4. Feldman JL, Baeza J, Denu JM (2013) Activation of the protein deacetylase SIRT6 by long-chain fatty acids and widespread deacylation by mammalian sirtuins. J Biol Chem 288(43):31350–31356
5. Du J, Zhou Y, Su X, Yu JJ, Khan S, Jiang H, Kim J, Woo J, Kim JH, Choi BH, He B, Chen W, Zhang S, Cerione RA, Auwerx J, Hao Q, Lin H (2011) Sirt5 Is a NAD-dependent protein lysine demalonylase and desuccinylase. Science 334(6057):806–809
6. Zhang Z, Tan M, Xie Z, Dai L, Chen Y, Zhao Y (2011) Identification of lysine succinylation as a new post-translational modification. Nat Chem Biol 7(1):58–63
7. Peng C, Lu Z, Xie Z, Cheng Z, Chen Y, Tan M, Luo H, Zhang Y, He W, Yang K, Zwaans BMM, Tishkoff D, Ho L, Lombard D, He T-C, Dai J, Verdin E, Ye Y, Zhao Y (2011) The first identification of lysine malonylation substrates and its regulatory enzyme. Mol Cell Proteomics 10 (12):M111.012658
8. Rardin Matthew J, He W, Nishida Y, Newman John C, Carrico C, Danielson Steven R, Guo A, Gut P, Sahu Alexandria K, Li B, Uppala R, Fitch M, Riiff T, Zhu L, Zhou J, Mulhern D, Stevens

Robert D, Ilkayeva Olga R, Newgard Christopher B, Jacobson Matthew P, Hellerstein M, Goetzman Eric S, Gibson Bradford W, Verdin E (2013) SIRT5 Regulates the mitochondrial lysine succinylome and metabolic networks. Cell Metab 18(6):920–933

9. Tan M, Peng C, Anderson Kristin A, Chhoy P, Xie Z, Dai L, Park J, Chen Y, Huang H, Zhang Y, Ro J, Wagner Gregory R, Green Michelle F, Madsen Andreas S, Schmiesing J, Peterson Brett S, Xu G, Ilkayeva Olga R, Muehlbauer Michael J, Braulke T, Mühlhausen C, Backos Donald S, Olsen Christian A, McGuire Peter J, Pletcher Scott D, Lombard David B, Hirschey Matthew D, Zhao Y (2014) Lysine glutarylation is a protein posttranslational modification regulated by SIRT5. Cell Metab 19(4):605–617
10. Nishida Y, Rardin Matthew J, Carrico C, He W, Sahu Alexandria K, Gut P, Najjar R, Fitch M, Hellerstein M, Gibson Bradford W, Verdin E (2015) SIRT5 regulates both cytosolic and mitochondrial protein malonylation with glycolysis as a major target. Mol Cell 59(2):321–332
11. Bao X, Wang Y, Li X, Li X-M, Liu Z, Yang T, Wong CF, Zhang J, Hao Q, Li XD (2014) Identification of 'erasers' for lysine crotonylated histone marks using a chemical proteomics approach. eLife 3:e02999
12. Park J, Chen Y, Tishkoff Daniel X, Peng C, Tan M, Dai L, Xie Z, Zhang Y, Zwaans Bernadette MM, Skinner Mary E, Lombard David B, Zhao Y (2013) SIRT5-mediated lysine desuccinylation impacts diverse metabolic pathways. Mol Cell 50(6):919–930
13. Nakagawa T, Lomb DJ, Haigis MC, Guarente L (2009) SIRT5 deacetylates carbamoyl phosphate synthetase 1 and regulates the urea cycle. Cell 137(3):560–570
14. Ogura M, Nakamura Y, Tanaka D, Zhuang X, Fujita Y, Obara A, Hamasaki A, Hosokawa M, Inagaki N (2010) Overexpression of SIRT5 confirms its involvement in deacetylation and activation of carbamoyl phosphate synthetase 1. Biochem Biophys Res Commun 393(1):73–78
15. Lin Z-F, Xu H-B, Wang J-Y, Lin Q, Ruan Z, Liu F-B, Jin W, Huang H-H, Chen X (2013) SIRT5 desuccinylates and activates SOD1 to eliminate ROS. Biochem Biophys Res Commun 441(1):191–195
16. Yu J, Sadhukhan S, Noriega LG, Moullan N, He B, Weiss RS, Lin H, Schoonjans K, Auwerx J (2013) Metabolic characterization of a Sirt5 deficient mouse model. Sci Rep 3:2806
17. Kumar S, Lombard DB (2014) Mitochondrial sirtuins and their relationships with metabolic disease and cancer. Antioxid Redox Signal 22(12):1060–1077
18. Sebastián C, Mostoslavsky R (2015) The role of mammalian sirtuins in cancer metabolism. Semin Cell Dev Biol. doi:10.1016/j.semcdb.2015.07.008
19. Lu W, Zuo Y, Feng Y, Zhang M (2014) SIRT5 facilitates cancer cell growth and drug resistance in non-small cell lung cancer. Tumor Biol 35(11):10699–10705
20. Borra MT, Smith BC, Denu JM (2005) Mechanism of human SIRT1 activation by resveratrol. J Biol Chem 280(17):17187–17195
21. Howitz KT, Bitterman KJ, Cohen HY, Lamming DW, Lavu S, Wood JG, Zipkin RE, Chung P, Kisielewski A, Zhang L-L, Scherer B, Sinclair DA (2003) Small molecule activators of sirtuins extend *Saccharomyces cerevisiae* lifespan. Nature 425(6954):191–196
22. Kokkonen P, Rahnasto-Rilla M, Mellini P, Jarho E, Lahtela-Kakkonen M, Kokkola T (2014) Studying SIRT6 regulation using H3K56 based substrate and small molecules. Eur J Pharm Sci 63:71–76
23. Madsen AS, Olsen CA (2012) Substrates for efficient fluorometric screening employing the NAD-dependent sirtuin 5 lysine deacylase (KDAC) enzyme. J Med Chem 55(11):5582–5590
24. Parenti MD, Grozio A, Bauer I, Galeno L, Damonte P, Millo E, Sociali G, Franceschi C, Ballestrero A, Bruzzone S, Rio AD, Nencioni A (2014) Discovery of novel and selective SIRT6 inhibitors. J Med Chem 57(11):4796–4804
25. Wegener D, Hildmann C, Riester D, Schwienhorst A (2003) Improved fluorogenic histone deacetylase assay for high-throughput-screening applications. Anal Biochem 321(2):202–208
26. Mercken EM, Mitchell SJ, Martin-Montalvo A, Minor RK, Almeida M, Gomes AP, Scheibye-Knudsen M, Palacios HH, Licata JJ, Zhang Y, Becker KG, Khraiwesh H, González-Reyes JA, Villalba JM, Baur JA, Elliott P, Westphal C, Vlasuk GP, Ellis JL, Sinclair DA, Bernier M, de Cabo R (2014) SRT2104 extends survival of male mice on a standard diet and preserves bone and muscle mass. Aging Cell 13(5):787–796
27. Mitchell Sarah J, Martin-Montalvo A, Mercken Evi M, Palacios Hector H, Ward Theresa M, Abulwerdi G, Minor Robin K, Vlasuk George P, Ellis James L, Sinclair David A, Dawson J, Allison David B, Zhang Y, Becker Kevin G, Bernier M, de Cabo R (2014) The SIRT1 activator SRT1720 extends lifespan and improves health of mice fed a standard diet. Cell Rep 6(5):836–843
28. Beher D, Wu J, Cumine S, Kim KW, Lu S-C, Atangan L, Wang M (2009) Resveratrol is not a direct activator of SIRT1 enzyme activity. Chem Biol Drug Des 74(6):619–624
29. Pacholec M, Bleasdale JE, Chrunyk B, Cunningham D, Flynn D, Garofalo RS, Griffith D, Griffor M, Loulakis P, Pabst B, Qiu X, Stockman B, Thanabal V, Varghese A, Ward J, Withka J, Ahn K (2010) SRT1720, SRT2183, SRT1460, and Resveratrol are not direct activators of SIRT1. J Biol Chem 285(11):8340–8351
30. Smith BC, Hallows WC, Denu JM (2009) A continuous microplate assay for sirtuins and nicotinamide-producing enzymes. Anal Biochem 394(1):101–109
31. Roessler C, Tüting C, Meleshin M, Steegborn C, Schutkowski M (2015) A novel continuous assay for the deacylase sirtuin 5 and other deacetylases. J Med Chem 58(18):7217–7223
32. Fischer F, Gertz M, Suenkel B, Lakshminarasimhan M, Schutkowski M, Steegborn C (2012) Sirt5 deacylation activities show differential sensitivities to nicotinamide inhibition. PLoS ONE 7(9), e45098
33. Roessler C, Nowak T, Pannek M, Gertz M, Nguyen GTT, Scharfe M, Born I, Sippl W, Steegborn C, Schutkowski M (2014) Chemical probing of the human sirtuin 5 active site reveals its substrate acyl specificity and peptide-based inhibitors. Angew Chem Int Ed 53(40):10728–10732
34. Li Y, Huang W, You L, Xie T, He B (2015) A FRET-based assay for screening SIRT5 specific modulators. Bioorg Med Chem Lett 25(8):1671–1674
35. Fan Y, Ludewig R, Imhof D, Scriba GKE (2008) Development of a capillary electrophoresis-based assay of sirtuin enzymes. Electrophoresis 29(18):3717–3723
36. Fan Y, Ludewig R, Scriba GKE (2009) 9-Fluorenylmethoxycarbonyl-labeled peptides as substrates in a capillary electrophoresis-based assay for sirtuin enzymes. Anal Biochem 387(2):243–248
37. Liu Y, Gerber R, Wu J, Tsuruda T, McCarter JD (2008) High-throughput assays for sirtuin enzymes: a microfluidic mobility shift assay and a bioluminescence assay. Anal Biochem 378(1):53–59
38. Ohla S, Beyreiss R, Scriba GKE, Fan Y, Belder D (2010) An integrated on-chip sirtuin assay. Electrophoresis 31(19):3263–3267
39. Abromeit H, Kannan S, Sippl W, Scriba GKE (2012) A new nonpeptide substrate of human sirtuin in a capillary electrophoresis-based assay. Investigation of the binding mode by docking experiments. Electrophoresis 33(11):1652–1659
40. Fan Y, Hense M, Ludewig R, Weisgerber C, Scriba GKE (2011) Capillary electrophoresis-based sirtuin assay using non-peptide substrates. J Pharm Biomed Anal 54(4):772–778
41. Pei J, Nie J, Kennedy RT (2010) Parallel electrophoretic analysis of segmented samples on chip for high-throughput determination of enzyme activities. Anal Chem 82(22):9261–9267

42. Perrin D, Frémaux C, Shutes A (2009) Capillary microfluidic electrophoretic mobility shift assays: application to enzymatic assays in drug discovery. Expert Opin Drug Discovery 5(1):51–63
43. Shanmuganathan M, Britz-McKibbin P (2013) High quality drug screening by capillary electrophoresis: a review. Anal Chim Acta 773:24–36
44. Guetschow ED, Steyer DJ, Kennedy RT (2014) Subsecond electrophoretic separations from droplet samples for screening of enzyme modulators. Anal Chem 86(20):10373–10379
45. DeLaMarre MF, Shippy SA (2014) Development of a simplified microfluidic injector for analysis of droplet content via capillary electrophoresis. Anal Chem 86(20):10193–10200
46. Niu X, Pereira F, Edel JB, de Mello AJ (2013) Droplet-interfaced microchip and capillary electrophoretic separations. Anal Chem 85(18):8654–8660
47. Niu XZ, Zhang B, Marszalek RT, Ces O, Edel JB, Klug DR, deMello AJ (2009) Droplet-based compartmentalization of chemically separated components in two-dimensional separations. Chem Commun 41:6159–6161
48. Roman GT, Wang M, Shultz KN, Jennings C, Kennedy RT (2008) Sampling and electrophoretic analysis of segmented flow streams using virtual walls in a microfluidic device. Anal Chem 80(21): 8231–8238
49. Wang M, Roman GT, Perry ML, Kennedy RT (2009) Microfluidic chip for high efficiency electrophoretic analysis of segmented flow from a microdialysis probe and in vivo chemical monitoring. Anal Chem 81(21):9072–9078
50. Harrison DJ, Fluri K, Seiler K, Fan Z, Effenhauser CS, Manz A (1993) Micromachining a miniaturized capillary electrophoresis-based chemical analysis system on a chip. Science 261(5123): 895–897
51. Roper MG, Shackman JG, Dahlgren GM, Kennedy RT (2003) Microfluidic chip for continuous monitoring of hormone secretion from live cells using an electrophoresis-based immunoassay. Anal Chem 75(18):4711–4717
52. Simpson PC, Roach D, Woolley AT, Thorsen T, Johnston R, Sensabaugh GF, Mathies RA (1998) High-throughput genetic analysis using microfabricated 96-sample capillary array electrophoresis microplates. Proc Natl Acad Sci U S A 95(5):2256–2261
53. Chabert M, Dorfman KD, de Cremoux P, Roeraade J, Viovy J-L (2006) Automated microdroplet platform for sample manipulation and polymerase chain reaction. Anal Chem 78(22):7722–7728
54. Pei J, Li Q, Lee MS, Valaskovic GA, Kennedy RT (2009) Analysis of samples stored as individual plugs in a capillary by electrospray ionization mass spectrometry. Anal Chem 81(15):6558–6561
55. Jacobson SC, Hergenroder R, Moore AW Jr, Ramsey JM (1994) Precolumn reactions with electrophoretic analysis integrated on a microchip. Anal Chem 66(23):4127–4132
56. Jacobson SC, Koutny LB, Hergenroeder R, Moore AW, Ramsey JM (1994) Microchip capillary electrophoresis with an integrated postcolumn reactor. Anal Chem 66(20):3472–3476
57. Shackman JG, Watson CJ, Kennedy RT (2004) High-throughput automated post-processing of separation data. J Chromatogr A 1040(2):273–282
58. Cosgrove MS, Bever K, Avalos JL, Muhammad S, Zhang X, Wolberger C (2006) The structural basis of sirtuin substrate affinity. Biochemistry 45(24):7511–7521
59. Inglese J, Johnson RL, Simeonov A, Xia M, Zheng W, Austin CP, Auld DS (2007) High-throughput screening assays for the identification of chemical probes. Nat Chem Biol 3(8):466–479
60. von Ahsen O, Bömer U (2005) High-throughput screening for kinase inhibitors. ChemBioChem 6(3):481–490
61. Schuetz A, Min J, Antoshenko T, Wang C-L, Allali-Hassani A, Dong A, Loppnau P, Vedadi M, Bochkarev A, Sternglanz R, Plotnikov AN (2007) Structural basis of inhibition of the human NAD+-dependent deacetylase SIRT5 by suramin. Structure 15(3): 377–389
62. Maurer B, Rumpf T, Scharfe M, Stolfa DA, Schmitt ML, He W, Verdin E, Sippl W, Jung M (2012) Inhibitors of the NAD+-dependent protein desuccinylase and demalonylase Sirt5. ACS Med Chem Lett 3(12):1050–1053
63. He B, Du J, Lin H (2012) Thiosuccinyl peptides as sirt5-specific inhibitors. J Am Chem Soc 134(4):1922–1925
64. Sun S, Kennedy RT (2014) Droplet electrospray ionization mass spectrometry for high throughput screening for enzyme inhibitors. Anal Chem 86(18):9309–9314
65. Suenkel B, Fischer F, Steegborn C (2013) Inhibition of the human deacylase sirtuin 5 by the indole GW5074. Bioorg Med Chem Lett 23(1):143–146
66. Su J, Chang C, Xiang Q, Zhou Z-W, Luo R, Yang L, He Z-X, Yang H, Li J, Bei Y, Xu J, Zhang M, Zhang Q, Su Z, Huang Y, Pang J, Zhou S-F (2014) Xyloketal B, a marine compound, acts on a network of molecular proteins and regulates the activity and expression of rat cytochrome P450 3a: a bioinformatic and animal study. Drug Des Devel Ther 8:2555–2602
67. Kainkaryam RM, Woolf PJ (2009) Pooling in high-throughput drug screening. Curr Open Drug Discov Dev 12(3):339–350

Erik Guetschow is a graduate student in the Department of Chemistry at the University of Michigan. His current research projects focus on interfacing nanoliter volume samples to microchip electrophoresis for high-throughput screening and in vivo chemical monitoring.

Surinder Kumar is a postdoctoral research fellow in the Lombard laboratory in the Department of Pathology at the University of Michigan. His current research projects are focused on exploring roles for the sirtuin SIRT5 in the regulation of cancer cell metabolism.

David B. Lombard is an Associate Professor in the Department of Pathology, and a Research Associate Professor in the Institute of Gerontology at the University of Michigan. His laboratory primarily focuses on sirtuin deacylases and their relationships with cancer and aging.

Robert Kennedy is a Distinguished University Professor and Chair of the Chemistry Department at the University of Michigan. His research interests are in the area of bioanalytical chemistry including separations, microfluidics, and mass spectrometry applied to endocrinology, neuroscience, and high throughput screening.